8

Mechanochemically Synthesized Metallic-Ceramic Nanocomposite; Mechanisms and Properties

M. Khodaei, M.H. Enayati and F. Karimzadeh
Department of Materials Engineering, Isfahan University of Technology, Iran

1. Introduction

Solid state chemical reaction is attributed to the chemical reaction performed at temperature which reactants are solid. In most solid state chemical reactions the reaction volume continually diminishes as the reactants become spatially separated by the products. As a result, the kinetics of solid state chemical reactions are limited by the rate at which reactant species are able to diffuse across phase boundaries and through intervening product layers. Hence, the conventional solid state technique invariably require the use of high processing temperatures to ensure that diffusion rate is maintained at a high level (Schmalzried, 1995), (Stein et al., 1993). On the other hand, high temperature process invariably leads to formation of coarse-grained products due to the occurrence of grain growth. Such coarse-grained materials are generally undesirable for manufacturing advanced engineering components due to their problems such as poor mechanical properties, poor sinterability, and etc. Consequently, there is considerable interest in alternative synthesis techniques that either reduce the required processing temperature or eliminate the need for applied heating altogether (McCormick, 1995), (McCormick & Froes, 1998).

Mechanical milling has been recognized as an effective way of occurrence the solid state chemical reaction at low temperature. This process is considered as a means to mechanically induced solid state chemical reaction that occur in precursors powder mixture during collision in the grinding media (Suryanarayana, 2001). Mechanical milling could be classified as mechanical grinding, mechanical alloying (MA), and Mechanochemical synthesis (MCS) according to the precursors powder mixture as well as structural and chemical changes that occur during milling. The milling process that there is no change in chemical composition of precursors is attributed to the mechanical grinding. The mechanical alloying is refers to the formation of alloys by milling of precursor materials. Finally, in mechanochemical synthesis process the chemical composition of precursors changes as a result of mechanically induced solid state reaction. This process is also termed as reactive milling (Suryanarayana, 2001), (Takas, 2002).

In this chapter book, the fundamental and mechanisms of mechanochemical process is presented and the recent developments in mechanochemically synthesized metallic-ceramic nanocomposite are overeviewed.

2. Milling equipments

Mechanical milling usually performed using ball milling equipments that generally divided to "low energy" and "high energy" category based on the value of induced the mechanical energy to the powder mixture. The ball milling equipments used for mechanical grinding or mixing are low energy such as Horizontal mill. In mechanical milling processes that utilize to change the chemical composition of precursors, the high energy ball milling equipments is generally used. Mechanochemical reaction can be performed in various types of high energy ball mills, including attrition, planetary, and vibratory mills that schematically shown in Fig. 1.

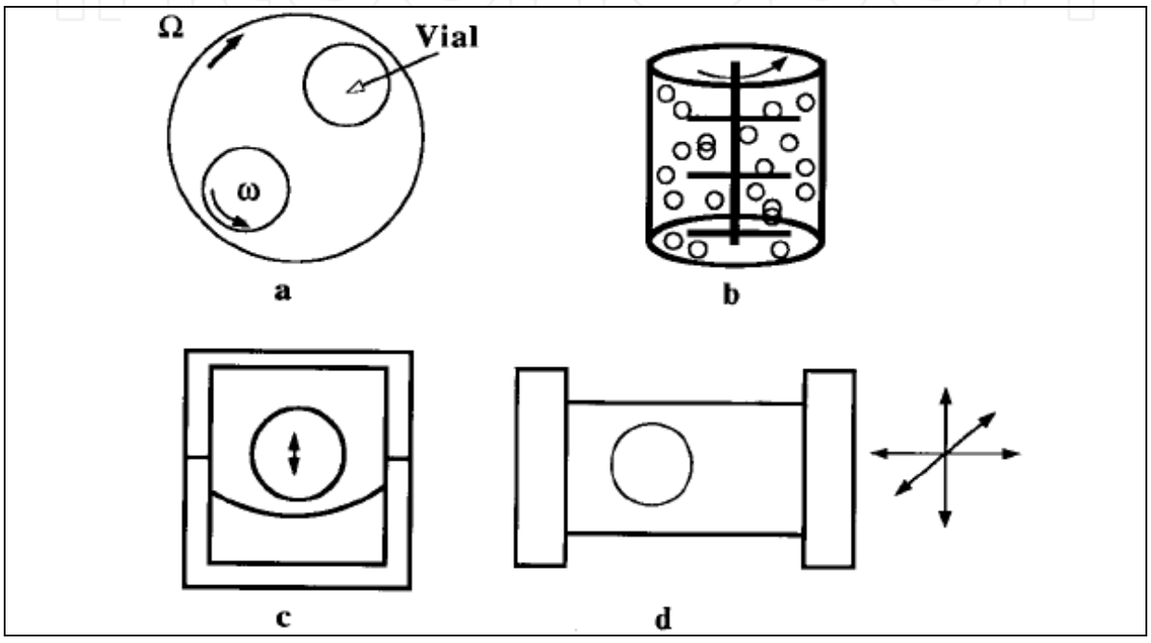

Fig. 1. Various types of high energy ball mills: (a) planetary mill, (b) attrition mill, (c) 1D vibratory mill, and (d) 3D vibratory mill (Suryanarayana, 2001).

In an attrition mill, the rotating impeller cause to relative movement between balls and powders. In a planetary ball mill, a rotating disc and vials revolve in opposite direction in order of several hundred rpm. A trade name of Fritsch is an example of the planetary mills. In a 1D vibratory mill that also known as a shaker mill, the vessel is set in vertical oscillatory motion. 3D vibratory mills consist of vials which shake at s frequency about 20 Hz in a "figure-eight" trajectory. Spex 8000 is a commercial type of 3D vibratory mills. The mechanical energy that induced by attrition mills is significantly lower that planetary or vibratory mills. However, unlike planetary and vibratory mills, attrition mills are readily amenable to scale up, which allows mass production of powders through mechanochemical process (Suryanarayana, 2001).

3. Reaction kinetics of mechanochemical synthesis

The mechanochemical reactions are characterized by a large negative free energy change at room temperature and are therefore thermodynamically feasible at room temperature. However, commercial operations by the pyrometallurgical techniques are conducted at

elevated temperature to overcome the kinetic barriers and achieve sufficiently high reaction rates whereas; mechanochemical process can be used more generally to promote chemical reactions. The underlying mechanism of mechanochemical process is repeated deformation, fracture, and welding of the powder charge during collisions of the grinding media. Fracture of particles exposes fresh reacting surfaces and welding generates interfaces between reactant phases across which short-range diffusion can occur, thus allowing chemical reactions to take place without kinetic constraint. Diffusion rates are also enhanced by the high concentration of lattice defects, which provide "short circuit" diffusion paths (Schaffer & McCormick, 1990), (Forrester & Schaffer, 1995).

Mechanochemical reaction could be done by two different reactions kinetics, "gradual" or "sudden" reaction, depending on nature of precursors (magnitude of enthalpy change during chemical reaction) as well as milling condition. If the enthalpy change associated with the formation of the product phases is low, then the heat generated will be insufficient to significantly influence the reaction kinetics. Therefore, reaction will proceed in a gradual manner. Gradual mechanochemical reaction systems have generally been found to exhibit sigmoidal reaction kinetics. The reaction rate initially increases with milling due to increasing activation and microstructural refinement of the reactants. The reaction rate then reaches a maximum at an intermediate milling time before decreasing as the reaction approaches completion due to dilution of the reactants by the product phases (Forrester & Schaffer, 1995). The sudden reactions take place as a self-propagating combustion reaction when the reaction enthalpy is sufficiently high. Combustion during milling is detected experimentally by the temperature spike associated with a sudden release of heat (Takacs, 2002). Fig. 2 shows the variation in temperature of a milling vial during processing of a highly exothermic reactant mixture. In the initial stages of milling, the temperature gradually increases up to a steady-state value as a result of heat generated by collisions of the grinding media. Following the critical milling time, depending on the milling condition for same precursors, the vial temperature suddenly increases due to the heat generated by combustion of the reactants. The temperature then slowly decays to the previous steady-state value.

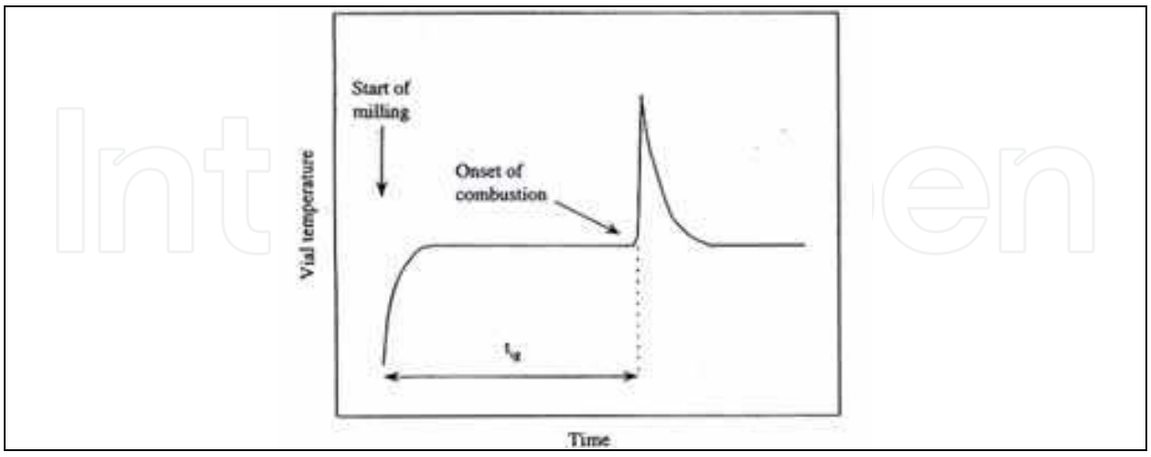

Fig. 2. Vial temperature as a function of time during milling of a combustive reaction system (Takacs, 2002).

Direct observation of ignition and propagation in mechanochemical combustion reaction during milling is also conducted by Deidda et al. (Deidda et al., 2004) using transparent

quartz vials. Fig. 3 shows the quartz vial at different time after starting the milling of the Ta:C=50:50 system. It is observed that the ignition begins after the initial time and then propagates. The local temperature of ignited powder is also recorded by pyrometer and presented as a function of milling time in Fig. 3.

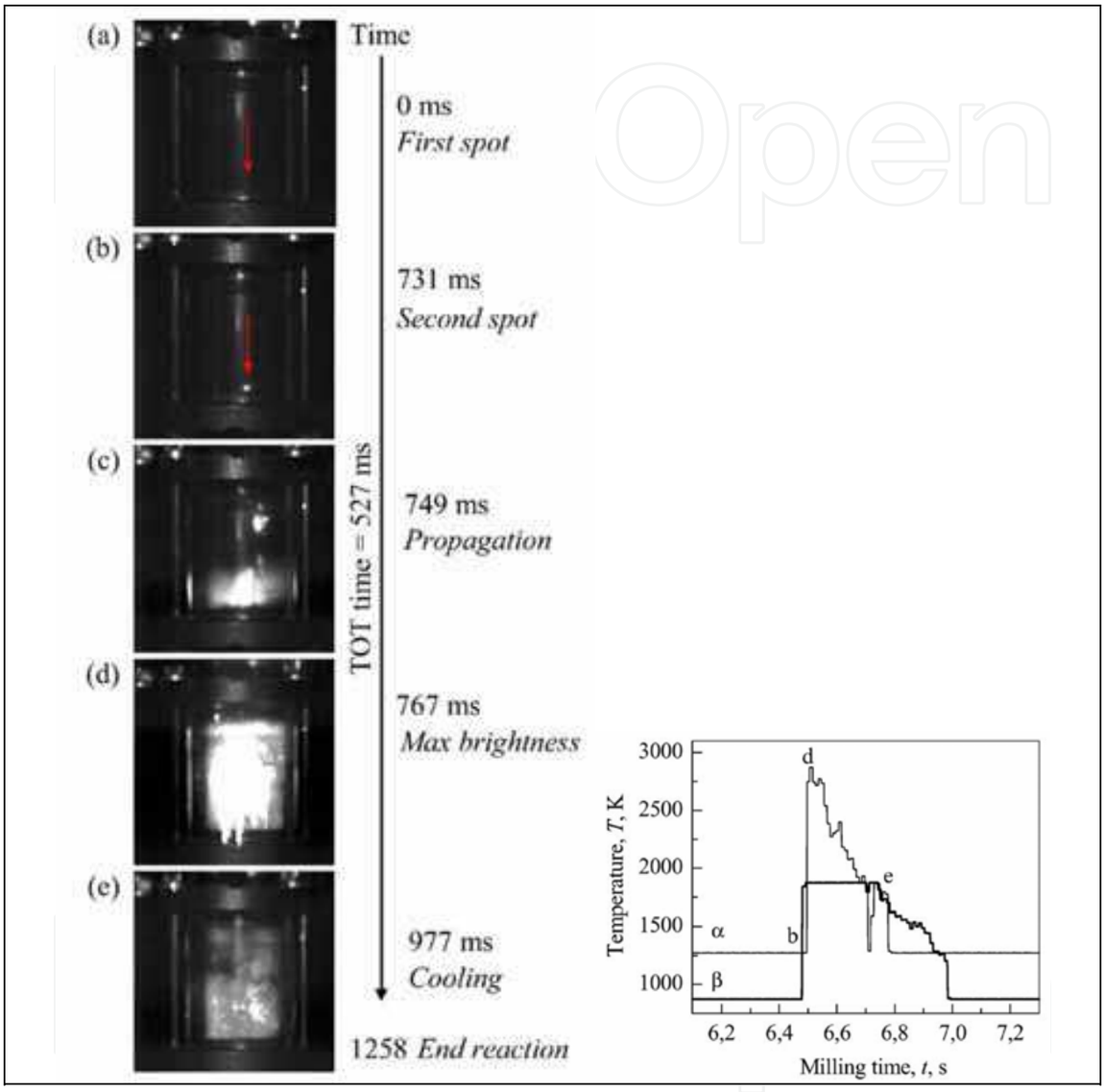

Fig. 3. High speed image sequence of the reaction of Ta:C=50:50 in a quartz vial coupled with the related temperature recording obtained by the infrared thermometer (Deidda et al., 2004).

The modality of displacement reactions can be specified by theoretical adiabatic temperature, T_{ad}, of the reaction. Tad represents the temperature of heat releasing during chemical reaction. A value of T_{ad}>1800K is generally considered to be the minimum necessary temperature for the occurrence of self-propagating combustion in a thermally ignited system (Munir, 1988). In contrast, Schaffer and McCormick (Schaffer & McCormick, 1990) showed that a value of T_{ad}>1300K is adequate for the sudden occurrence of chemical reaction during ball milling. The Tad value could be estimated from the following relation:

$$\Delta H_r + \sum \int_{T_i}^{T_m} {}^{s}C_p + \sum \Delta H_t + \sum \int_{T_m}^{T_{ad}} {}^{l}C_p = 0 \quad (1)$$

Where ΔH_r is the heat of reaction, T_i is the initial temperature, the T_m's are the melting points of products, the ${}^{s}C_p$'s are the molar heat capacities of the solid products, ΔH_t's are the heat of transitions of the products and ${}^{l}C_p$'s are the molar heat capacities of the liquid products. It should be noted that the last term in relation 1 is ignored if $T_{ad} < T_m$'s.

The experimental combustion temperature for several systems (recorded by pyrometer technique (Deidda, 2004)) and theoretical T_{ad} are presented in Table 1. As seen, the pyrometer recorded temperature of combustion reaction during milling is invariably close to the calculated T_{ad}.

Chemical system	Adiabatic temperature, T_{ad} (K)	Combustion temperature, T_c (K)
Ti_5Si_3	2550	2420
$TiSi$	2370	1818
Ti_5Si_4	2193	2063
$TiSi_2$	1829	1613
$Ti_{70}C_{30}$	1991	2183
$Ti_{60}C_{40}$	2614	2773
$Ti_{50}C_{50}$	3206	>2873
$Ta_{50}C_{50}$	2901	2870

Table 1. The experimental combustion temperature and the calculated adiabatic temperature for the various systems (Deidda et al., 2004).

4. Mechanochemical synthesis

It was recognized in 1989 that ball milling could be used to induce a solid state chemical reaction by demonstrating that the pure metal Cu can be synthesized when CuO and Ca were ball milled together at room temperature. Simultaneous reduction of CuO and ZnO by Ca has also been shown to result in the formation of brass (Schaffer & McCormick, 1989), (McCormick et al., 1989). After that the extensive researches for preparing other metals such as Fe, Ti, Zr, W, and etc. were performed. The mechanochemical reactions could be divided to two categories involve non-displacement and displacement chemical reactions. Non-displacement reactions are the chemical reaction occurred in the reactants in order to combine the elements to produce final phases. This process is similar to mechanical alloying. In displacement reaction, the reactants react to each others with exchange the element between them to form new phases. Most of the mechanochemical reactions studied have been displacement reactions of the type:

$$MO + R \rightarrow M + RO \quad (2)$$

Where a metal oxide (MO) is reduced by a more reactive metal (reductant, R) to the pure metal M. Metal chlorides and sulfides have also been reduced to pure metals this way. The products of displacement reactions normally consist of two phases, the metal (or a compound) and the oxide, chloride, or sulfide associated with the reactant. For preparing pure metallic phase, the by–product must be removed by removal processes such as

leaching. The removal of one of the phases produced by mechanochemical reaction may be difficult due to the high reactivity of the metallic phase associated with nanocrystalline structure and intermixing of the phases induced by mechanical forces (El-Eskandarany, 2001a). Therefore, utilizing the products of mechanochemical reaction to fabricate the composite structures could be useful to change the properties of each phase. Since, unlike chlorides and sulfides, the oxide phases could be used in structural application, the most mechanochemical reactions to synthesize composite structure have been used the reduction of oxide phase. Mechanochemically synthesized component with more than two phases offers a number of advantages over the conventional metal processing techniques. First it is enable to reduce a number of oxides and halides to desired compound at room temperature, thus it is cost effective. Second, if a number of components are reduced simultaneously, then it is possible to produce an alloy without first having to convert the oxides to pure metals and then to desired alloy. Third, for powder metallurgy application, it allows the direct formation of powder product. Fourth, severe plastic deformation induced during high energy ball milling cause to formation of nanocrystalline structure. Finally, the mechanochemically synthesized phases especially trough displacement reaction are chemically compatible (Suryanarayana, 2001), (Takacs, 2002).

Recently, synthesis of metallic-ceramic composite powder through mechanochemical reaction is considered because of advantages mentioned above. In this area, the ceramic (metallic) phase especially considered as reinforcement (tougher) for metallic (ceramic) phase to enhance its properties. This chapter presents an overview of the recent developments in mechanochemically synthesized metallic-ceramic nanocomposite consist of metal-ceramic and Intermetallic-ceramic trough displacement reaction.

4.1 Metal-ceramic nanocomposite

It is well known that the addition of hard ceramic particles to soft metals provides a combination of properties of both metallic matrix and ceramic reinforcement components. This may result in improvement of physical and mechanical properties of the composite (Rajkovic et al., 2008).

Many methods were studied to prepare metal-based composites. The one of methods for preparation of metal-base composite is casting. In this method, particles are added to molten metal by stirring before casting. However, the difference in thermal expansion coefficients between ceramic particles and molten metal constituents and the poor wettability between these two become an obstacle to the liquid method used for synthesizing metal matrix composite (Konopka & Szafran, 2006). Another way of producing both metal-based and ceramic-based composite is using powder metallurgy methods. In powder metallurgy methods, the composite powder is consolidated to producing composite part. In these methods, the powder could be prepared by mixing or reaction of constituents. The preparation of composite powder by mechanochemical reaction is expected an advanced method for fabrication of nanocrystalline part (El-eskandarany, 2001a)

One of the first reports on mechanochemical synthesis of metal-ceramic nanocomposite has been published by Matteazzi and Caer about alumina-iron nanocomposite powders produced by mechanochemical reaction between hematite and aluminum (Matteazzi & Caer, 1992). The mechanochemical reduction of copper oxide with different reductants such as Fe, Al, Ti, Ca, Ni and C has been investigated (Schaffer & McCormick, 1990), (Schaffer & McCormick, 1991). Their products were often a mixture of copper with dispersed oxides particle, i.e. copper matrix composites such as Cu–Al_2O_3 (Wu & Li, 2000), (Ying & Zhang, 2000), (Hwang et al.,

2004) (Hwang & Lee, 2005), Cu–ZnO (Hessel et al., 2001), and Cu–MnO (sheibani et al., 2009). One of the most important ceramic particles used in structural application is Al_2O_3 (Ying & Zhang, 2000), (Hwang & Lee, 2005). The presence of fine Al_2O_3 articles in copper matrix leads not only to improve the hardness of this material, but also to decrease the grain growth rate at temperatures even close to the melting point of copper matrix. In this way, the amount, size and distribution of reinforcing particles play a critical role in enhancing or limiting the overall properties of the composite (Rajkovic et al., 2008). Hwang et al. (Hwang et al., 2004) (Hwang & Lee, 2005) synthesized Cu-Al_2O_3 nanocomposite powder by mechanochemical reaction between Cu_2O and Al according to the following reaction:

$$3Cu_2O + 2Al + XCu \rightarrow (6+X)Cu + Al_2O_3$$

The presence of Cu in the precursor powder mixture lead to formation of different amount of Al_2O_3 in the range of 4 to 21 volume percent. XRD pattern of powder mixture as-received and after different milling time are show in Fig. 4.

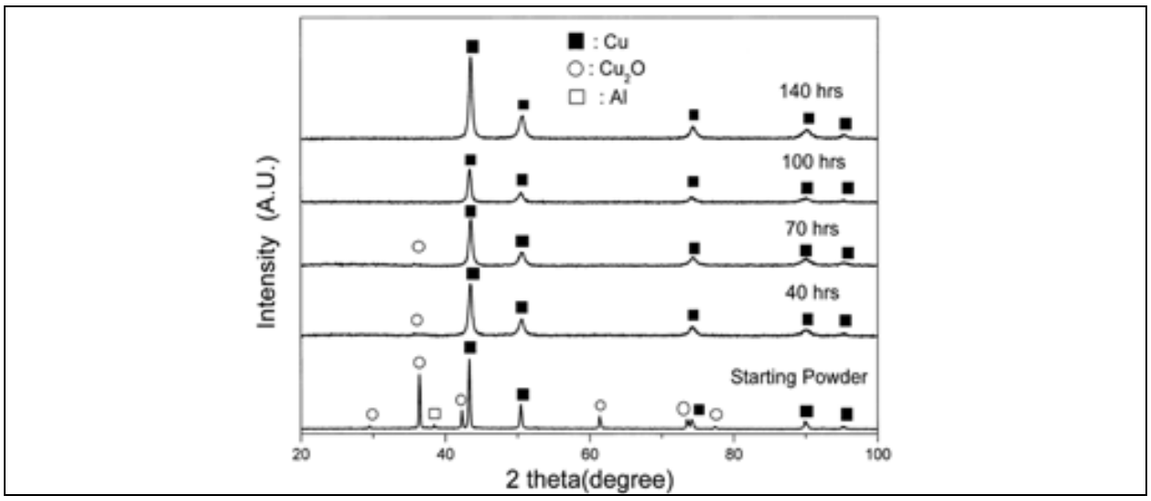

Fig. 4. XRD pattern of Cu_2O+Al+Cu powder mixture as-received and after different ball milling time (Hwang et al., 2004).

As can be seen, the Cu_2O peaks reduced and only the peaks related to the Cu is remained after milling. There is also no evidence of Al_2O_3 phase on XRD pattern that attributed to the peak broadening as a result of nanocrystalline or highly strained powder.

Transmission Electron microscopy (TEM) of prepared powder after 140 h ball milling was performed for further investigation. Fig. 5 shows TEM bright field (Fig. 5a), dark field (Fig. 5b) and Selected Area Diffraction (SAD) pattern (Fig. 5c) obtained from a small particle of the nanostructural powder after milling for 140 h.

Typical SAD patterns displayed spotty rings which could be indexed as a mixture of FCC Cu and Rhomboheral α-Al_2O_3. The fine structure of the spotty rings indicated that both Cu and α-Al_2O_3 phases took the form of predominantly nanostructural particles. Dark field imaging confirmed this and indicated a bimodal size distribution of nanocrystallites, with an average size of around 2–5 nm for the smaller crystals and around 10–20 nm for the larger ones. A TEM-energy dispersive spectroscopy (EDS) micrograph of the hot pressed samples contained 21 vol.% Al_2O_3 is given in Fig. 6 along with EDS spectra of the dark and bright phases. EDS spectra collected from the phases show that the dark phase is Cu while

the bright phase is Al_2O_3. The crystallite size of both phases in hot pressed 21 vol.% Al_2O_3 sample at different pressing temperatures (800 to 900 °C) reported in the range of 20 to 30 nm. The results of Rockwell hardness tests of hot pressed samples with different vol.% Al_2O_3 (from 4.1 to 20.9) are given in Table 2. The hardness of the hot pressed samples increases from 70 to 103 HRB with increasing vol.% of Al_2O_3. The hardness of the samples is in reasonable proportion to the vol.% of Al_2O_3 formed in Cu matrix.

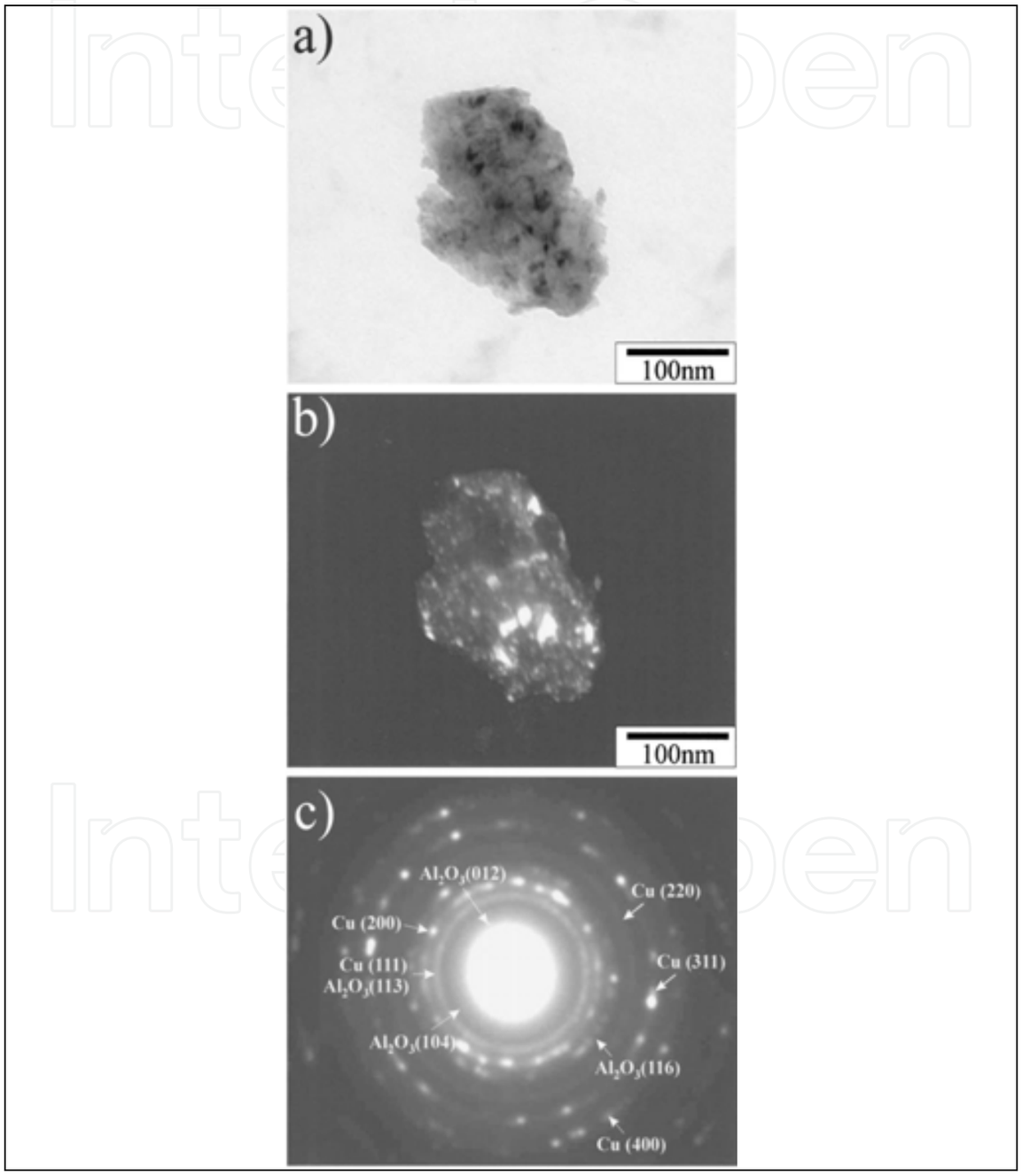

Fig. 5. TEM images of nanostructural Cu-21 vol.% Al_2O_3 powder particle after 140 h milling time, (a) bright field image, (b) dark field image and (c) SAD pattern (Hwang et al., 2004).

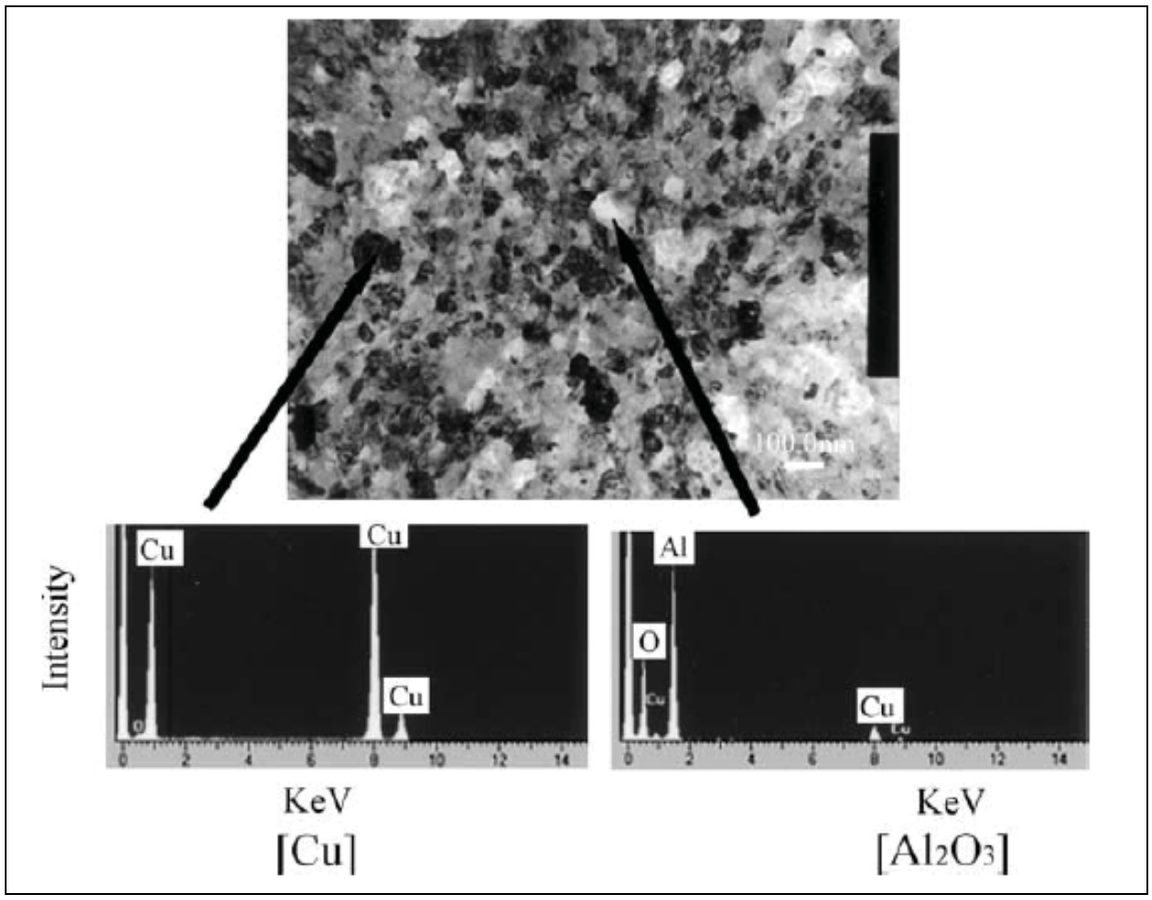

Fig. 6. TEM bright field image and energy dispersive spectroscopy (EDS) micrograph of the hot pressed Cu- 21 vol.% Al_2O_3 sample (Hwang & Lee, 2005).

Alloy	Hardness number (HR_B)
HP-4.1	70 ± 4
HP-11.9	88 ± 2
HP-15.5	98 ± 3
HP-20.9	103 ± 1

Table 2. Rockwell hardness test on the hot pressed samples at 850 ◦C with different vol.% Al_2O_3 from 4.1 to 20.9 (Hwang & Lee, 2005).

It is also reported that a common way of increasing the low intrinsic strength of Cu is alloying with BCC elements such as Mo (Botcharova et al., 2004). Sabooni et al. synthesized the Cu–15Wt.%Mo/30Vol.%Al_2O_3 (Cu(Mo)-Al_2O_3) nanocomposite by mechanochemical reaction between MoO_3 and Al in presence of Cu (Sabooni et al., 2010). The modality of mechanochemical reaction in MoO_3+Al and MoO_3+Al+Cu powder mixture are determined as combustion mode according to the calculated T_{ad} as well as measured vial temperature. Fig. 7 shows the vial temperature during milling for MoO_3+Al (without diluent) and MoO_3+Al+Cu (with Cu as diluent) powder mixture. The presence of Cu leads to decrease the T_{ad} of MoO_3+Al reaction from 4773 to 2361 K and increase the combustion time.

The crystallite size of Cu in Cu(Mo)-Al_2O_3 calculated from XRD pattern using Williamson–Hall method after 60 h ball milling and subsequent annealing were reported about 30 and 50-80 nm, respectively. TEM images of 60 h milled powder presented in Fig. 8 reveal a homogenous dispersion of reinforcements with the size of about 10nm in the matrix. TEM images also approve the nanocrystalline structure of the matrix which had been obtained by Williamson–Hall method. The average microhardness values of pure Cu (Sabooni et al., 2010) and nanostructured Cu (Chen et al., 2006) increases from 39HV to 178 HV as a result of decreasing in crystallite size.

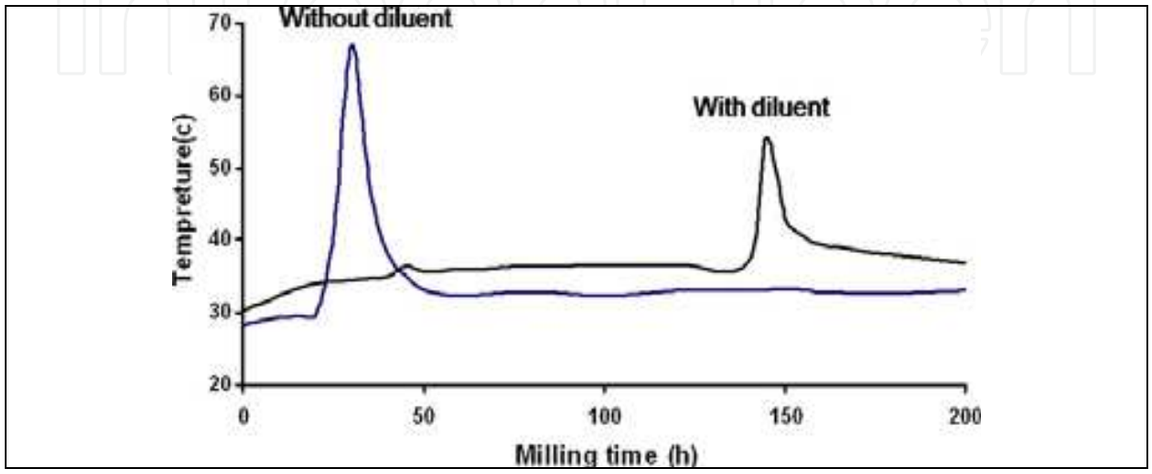

Fig. 7. Vial temperature as a function of milling time (minute) (Sabooni et al., 2010).

Addition of alloying element of Mo in order to have nanocrystalline solid solution leads to increase hardness to about 198 HV in Cu(Mo) (Sabooni et al., 2010). Finally, incorporation of ceramic nanoparticles in a nanocrystalline matrix of Cu(Mo) leads to high increase of hardness to 307HV in Cu(Mo)-Al_2O_3 (Sabooni et al., 2010) which is about eight times higher than the hardness of pure Cu. Three important strengthening mechanisms are suggested for high value of hardness in Cu(Mo)-Al_2O_3 nanocomposite: reduction of crystallite size, formation of Cu(Mo) solid solution and dispersion hardening of nanometric reinforcements in the nanocrystalline matrix.

Aluminum-based composites are ideal materials for structural applications in the aerospace and automotive industries due to their high strength-to-weight ratio (Clyne & Withers, 1995). Reinforcing the ductile aluminum matrix with stronger and stiffer second-phase reinforcements such as oxides, carbides, borides, and nitrides provides a combination of properties of both the metallic matrix and the ceramic reinforcement components (Piggott, 1980). In recent years, many researchers have paid attention to new fabrication techniques for making aluminum matrix composite. Synthesis of Al based nanocomposites by mechanochemical reaction has recently been examined by some researchers. Shengqi et al. have investigated the mechanochemical reaction of CuO and Al powder (Shengqi et al., 1998). Wu and Li have synthesized nanostructured aluminum matrix composite reinforced with $CuAl_2$ (100–500 nm in size), Al_2O_3 and Al_4C_3 (10–50 nm in size) (Wu & Li, 2000). The solid reactions between CuO and Cu–14 at.%Al alloy or Cu_9Al_4 inermetallic compound during high energy mechanical milling to produce Cu-Al/Al_2O_3 have been studied (Ying & Zhang, 2003). Arami et al. (Arami et al., 2008) synthesized the Al(Cu)-Al_2O_3 nanocomposite through gradual mechanochemical reaction because of nonstoichiometric composition of

CuO and Al (Al–5.8 wt.%CuO). TEM image and corresponding EDS analysis of Al–CuO powder mixture milled for 60 h is shown in Fig. 9. Nanometric alumina particles, mostly located at the grain boundaries, could be seen in Fig. 9.

Al(Ce)-Al_2O_3 nanocomposite is also fabricated by mechanochemical reaction in Al-CeO powder mixture (Reddy, 2007). Tavoosi et al. have also reported the formation of Al–13.8 wt%Zn-5 vol%Al_2O_3 (Al(Zn)-Al_2O_3) nanocomposite by mechanochemical reaction of Al-ZnO powder mixture followed by hot pressing (Tavoosi et al., 2008), (Tavoosi et al., 2009). The crystallite, relative density, and hardness of hot pressed samples with and without Al_2O_3 at different temperature are presented in Table 3.

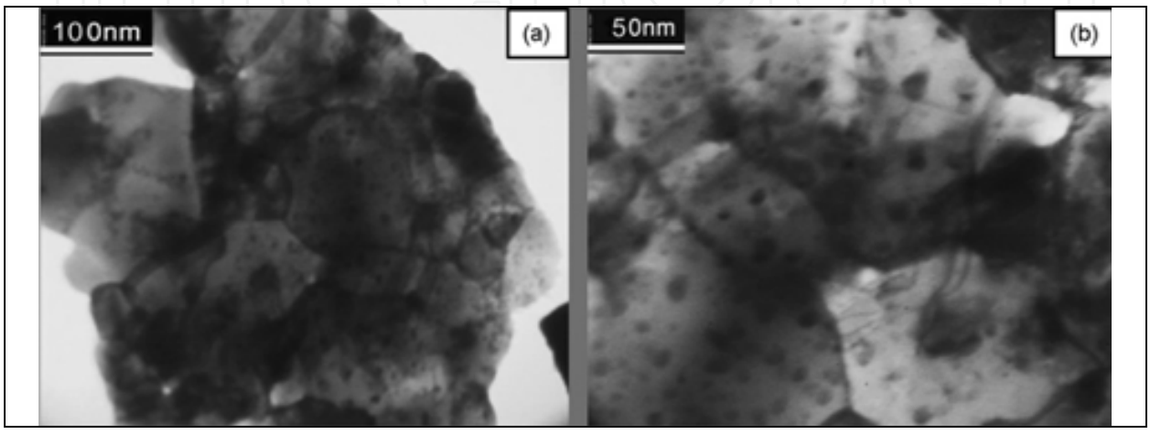

Fig. 8. TEM bright field image of 60 h ball milled MoO_3+Al+Cu powder mixture to produce Cu(Mo)-30 Vol.%Al_2O_3 nanocomposite at two magnifications (Sabooni et al., 2010).

Fig. 10 shows the hardness changes of bulk Al–13.8 wt%Zn-5 vol%Al_2O_3 and Al–13.8 wt%Zn vs. annealing time at different temperatures. As can be seen from this figure, the hardness value for Al–13.8 wt%Zn-5 vol%Al_2O_3 after annealing at 200 and 400 C remained constant. However, annealing at 500 C for longer times causes grain growth and therefore a decrease in hardness value. The Al–13.8 wt%Zn-5 vol%Al_2O_3 is more stable than Al–13.8 wt%Zn because of the effect of 5 vol%Al_2O_3 nano-particles in the matrix (Tavoosi et al., 2009).

El-Eskandarany et al. synthesized Fe-MgO by mechanochemical reaction of Fe_2O_3 and Mg (El-Eskandarany et al., 2001). Co-Al_2O_3 nanocomposite is also prepared by mechanochemical reduction of CoO by Al. The average grain sizes of the nanocomposite powders are reported 19 nm for Co and 28 nm for Al_2O_3 after the completion of the reduction reaction (Li et al., 2007). Karimzadeh et al. also reported the synthesis of Zn-Al_2O_3 by mechanochemical reaction between ZnO and Al. The microhardness value of produced nanocomposite powder was about 350HV which was 10–15 times higher than the microhardness of pure zinc (20–30 HV) (Karimzadeh et al., 2008).

Samples	Temperature (°C)	Relative density (%) (S.D. 0.5%)	Hardness (HV)	Crystallite size (nm)
Al–13.8 wt%Zn/5 vol%Al_2O_3	400	95	150	40
	500	99.6	185	40
Al–13.8 wt%Zn	400	96	120	40
	500	99.8	150	40

Table 3. Relative density, hardness and crystallite size of bulk Al–13.8 wt%Zn-5 vol%Al_2O_3 and Al–13.8 wt%Zn (Tavoosi et al., 2009).

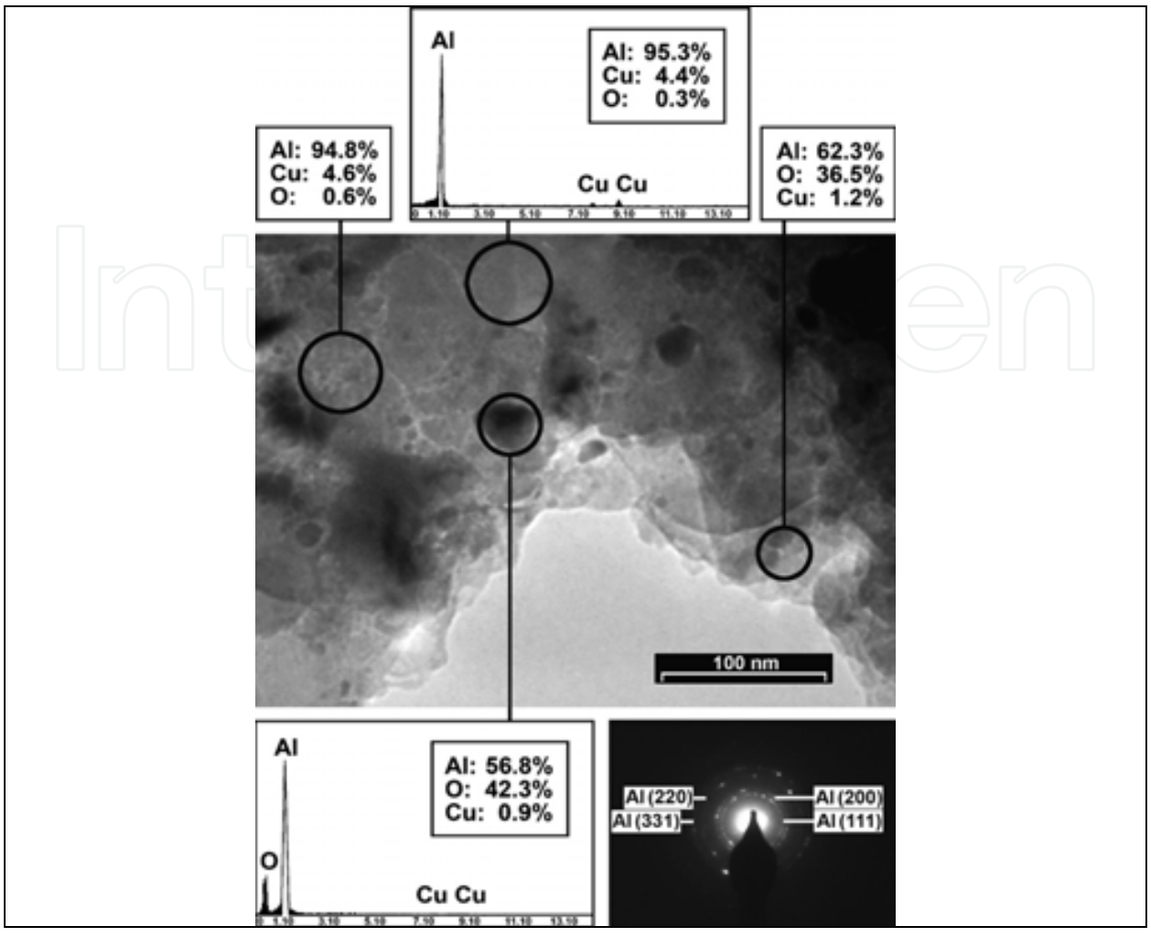

Fig. 9. TEM (bright field) image, EDS analysis and SAD pattern of Al–CuO powder mixture after 60 h ball milling (Arami et al., 2008).

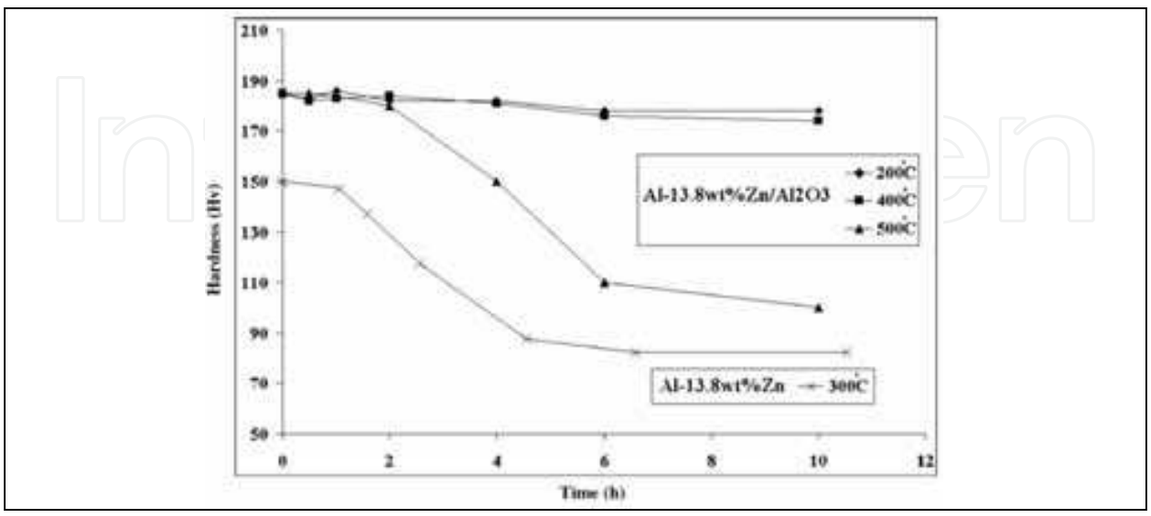

Fig. 10. The hardness changes of Al–13.8 wt%Zn-5 vol%Al_2O_3 and Al–13.8 wt%Zn vs. annealing times at different temperatures (Tavoosi et al., 2009).

The presence of metallic particles in ceramics adds physical properties inherent to the metallic phase, such as electric and thermal conductivity or magnetic properties. This combination of properties makes ceramics – metals composite excellent candidates for electric, optic, and magnetic devices or chemical sensors. Some properties such as toughness and wear behavior of ceramic – metal composites are expected to be improved in compare to monolithic ceramic phase (Chalwa, 1993). So, fabrication of ceramic matrix nanocomposite can strongly improve the room temperature toughness and high temperature strength of ceramics (Mishra & Mukherjee, 2001). Matteazzi and Caer synthesized nanometer-sized $A1_2O_3$–M composite (M= Fe, V, Cr, Mn, Co, Ni, Cu, Zn, Nb, Mo, W, Si) by mechanochemical reaction of an appropriate metal oxide and (Matteazzi & Caer, 1992). Recently, Heidarpour et al. synthesized Al_2O_3-Mo nanocomposite with different volume persent of Mo (Heidarpour et al., 2009). Mostaan et al. also reported for the first time on mechanochemical reaction in Nb_2O_5+Al powder mixture to synthesizing Al_2O_3-Nb nanocomposite (Mostaan et al., 2010a). They investigated the reaction mechanism and activation energy (E_a) of aluminothermic reaction between Al and Nb_2O_5 under non-isothermal conditions using XRD and differential thermal analysis (DTA). It was found that the mechanically milled Al–Nb_2O_5 powder mixture was converted to Al_2O_3-Nb composite in three stages and during the reduction intermediate Nb oxides (NbO_2 and NbO) were formed (Mostaan et al., 2010c).

4.2 Intermetallic-ceramic nanocomposite

Intermetallic compound is an important class of materials because of a combination of its high tensile strength, low density, good wear resistance, and creep resistance. These properties have led to the identification of several potential usages including structural applications and protective coatings (Sauthoff, 1995). Two major problems that restrict the application of Intermetallic are poor low-temperature ductility and inadequate high-temperature creep resistance. These limitations can be overcome by introducing ceramic particles as reinforcements (Morris, 1998). Originally, reinforcement phase can be introduced in the matrix by two routs namely ex-situ addition of reinforcement particles and in-situ formation of reinforcement phase via a displacement reaction which both phase (Intermetallic and ceramic) are formed during ball milling. The later route can be done by mechanochemical process which has an advantage over other fabrication route because of its capability of producing chemical compatible phase as well as nanosized structure with high uniformity. The important Intermetallic compound is NiAl, FeAl, TiAl, and NiTi that mechanochemically synthesized intermetallic-ceramic nanocomposite were overeviewed.

Development of NiAl–Al_2O_3 nanocomposites by mechanical milling has been achieved by the milling of Ni–Al–Al_2O_3 (lin et al., 2000) and NiO–Al powder mixture (Oleszak, 2004), (Anvari et al., 2009), (Udhayabanu et al., 2010). In order to fabricate the Ni_3Al- or NiAl-based composite via mechanochemical displacement reaction, the nickel oxide (NiO) could be used to reduce by aluminum according to the following reactions:

$$3NiO + 3Al \rightarrow Ni_3Al + Al_2O_3 \quad (4)$$

$$3NiO + 5Al \rightarrow NiAl + Al_2O_3 \quad (5)$$

The first report on synthesis of NiAl-Al_2O_3 nanocomposite by mechanochemical reaction of stoichiometric 3NiO+5Al powder mixture was reported by Oleszak (Oleszak, 2004). XRD

pattern of 3NiO+5Al powder mixture as-received and after different ball milling time are presented in Fig. 11. XRD pattern of 3NiO+5Al powder mixture as-received and after 1 h milling time show the peaks corresponding the NiO and Al phases whereas the XRD pattern of 1.5 h ball milled sample indicates the formation of NiAl and Al_2O_3 phases. The crystallite size and lattice strain of phases measured from XRD pattern using Williamson-Hall Method were reported in the range of 40-50 nm and 0.4% for 2 h milled and 10-20 nm and 0.9% for 4 h milled samples.

Anvari et al. was investigated the mechanochemical reaction of NiO–38 wt% Al and NiO–34wt% Al–41 wt% Ni in order to give the final product NiAl–Al_2O_3 composite with 40 and 20 vol.% contribution of alumina, respectively (Anvari et al., 2009). They reported that NiAl–40 vol.% Al_2O_3 nanocomposite formed by a combustion reaction. In contrast for NiAl–20 vol.% Al_2O_3 high exothermic reaction did not occur during the milling process, due to the presence of Ni content in initial mixture. Increasing Ni concentration increased the start time of NiAl and Al_2O_3 formation, and changed the morphology of products. XRD patterns of NiO+Al and NiO+Al+Ni powder mixtures as-received and after different milling times are shown in Fig. 12 and 13, respectively. As can be seen, the NiAl and Al_2O_3 phases were synthesized in both samples during milling.

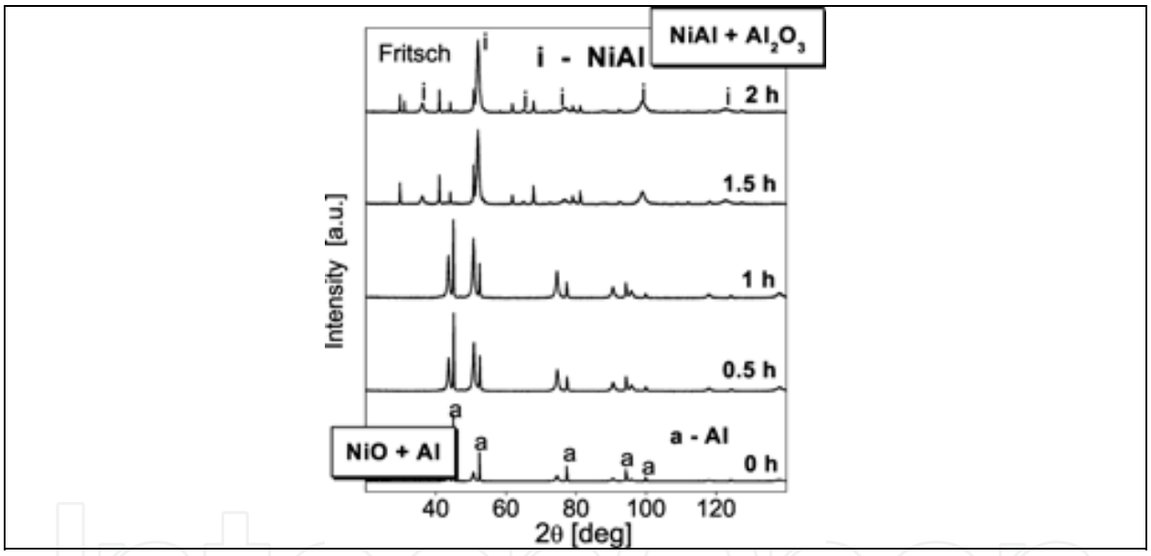

Fig. 11. XRD pattern of 3NiO+5Al powder mixture as-received and after different ball milling time (Oleszak, 2004).

Udhayabanu et al. also synthesized nanocrystalline NiAl based nanocomposite with 30 vol.% of Al_2O_3 by carrying out milling of NiO, Al, and Ni powder mixture in toluene medium for 20 h followed by heating. They reported NiAl phase formation and NiO reduction occur gradually and simultaneously during milling. Small amount of NiO which remains unreacted in 20 h milling got reduced at 420 °C on heating. Small amount of Ni_3Al phase is also formed as intermediate product and it later transforms to NiAl phase above 900 °C on heating. The amorphous alumina is formed as the product of the NiO reduction by Al and it transforms to stable α-Al_2O_3 at 1000 °C via the formation of metastable transition γ-Al_2O_3. The TEM results revealed that the α-Al_2O_3 particles are 11±3 nm in size and the average crystallite size of NiAl phase is 115±40 nm in the 20 h milled powder after heating to 1120 °C.

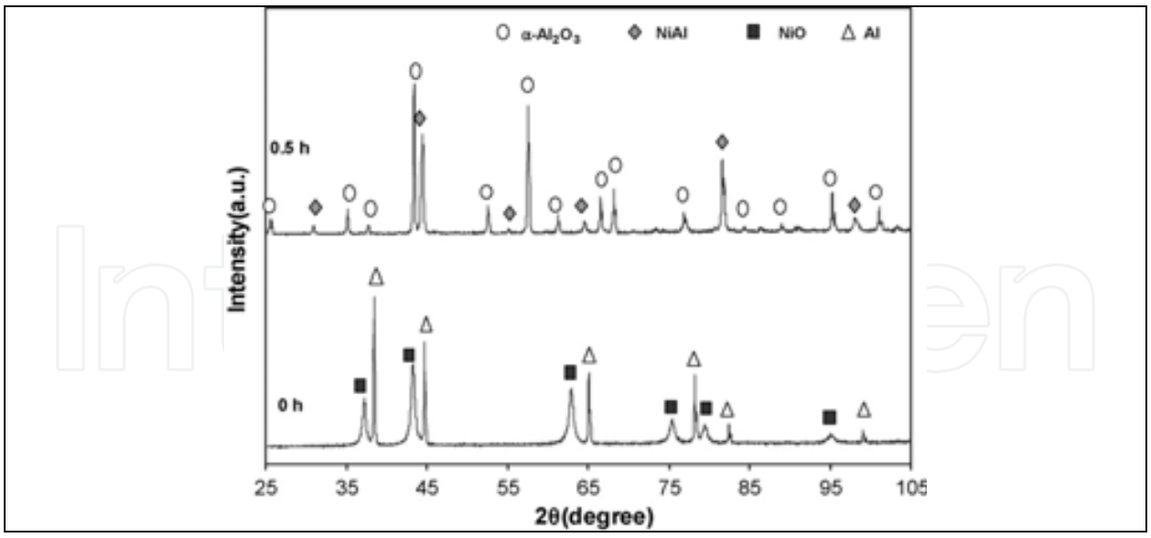

Fig. 12. XRD patterns of NiO–38 wt% Al powder mixtures as-received and after milling for 0.5 h (Anvari et al., 2009).

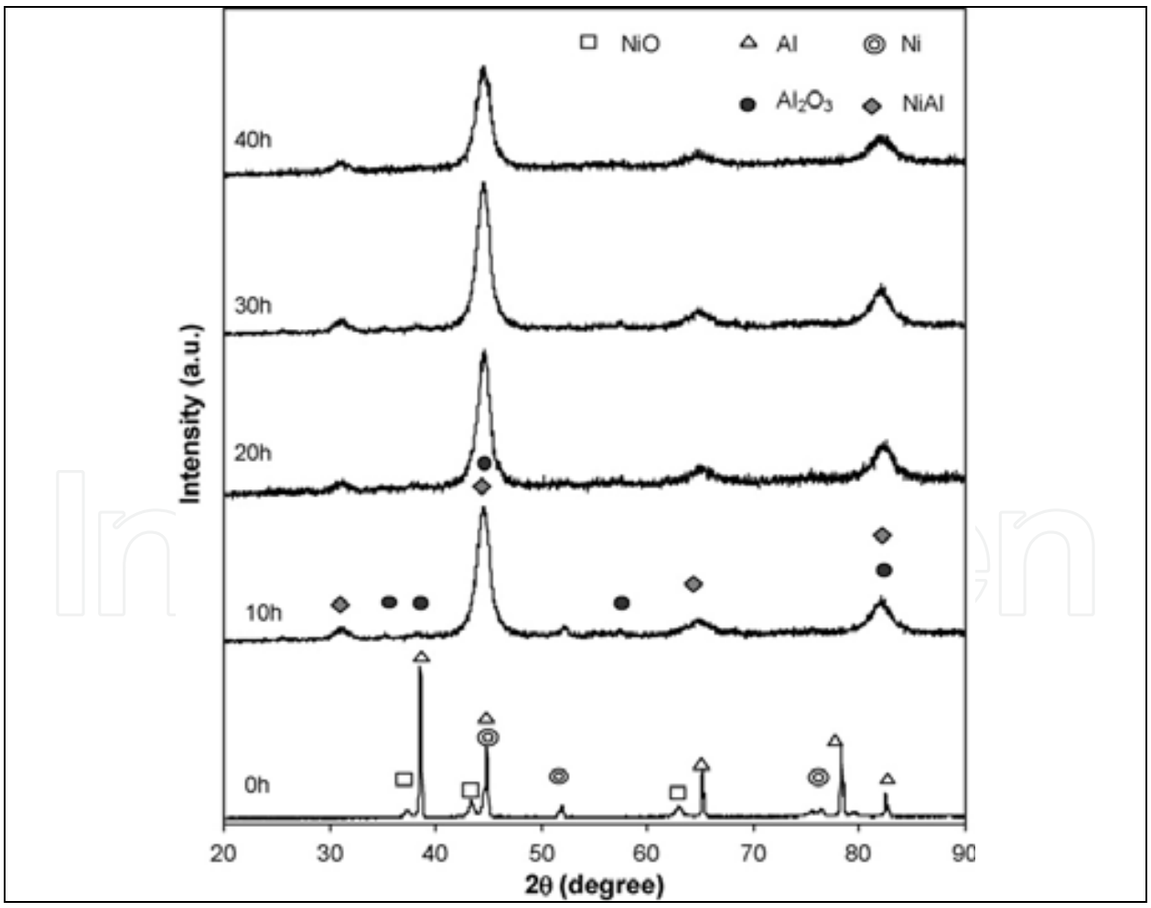

Fig. 13. XRD traces of NiO–34 wt% Al–41 wt% Ni powder mixtures as-received and after different milling times (Anvari et al., 2009).

Mousavi et al. reported the Synthesis of NiTi-Al_2O_3 nanocomposite by mechanochemical reaction of a powder mixture containing NiO, Al, Ti and Ni. They also reported the combustion mechanochemical reaction between NiO and Al leading to the formation of nanocomposite for this dialued system in presence of Ni and Ti (Mousavi et al., 2009).
Iron aluminides compound, especially FeAl and Fe_3Al compounds, possess a combination of attractive physical, thermal and mechanical properties including low density, high tensile strength, good oxidation, corrosion, and sulfidation resistance. These properties along with low cost make iron aluminides potentially useful for structural and coating applications (Sauthoff, 1995). Incorporation of ceramic reinforcement in iron aluminides lead to enhance the high temperature strength (Subramanaian et al., 1997), (Subramanaian et al., 1998) as well as wear resistance of iron aluminides (Alman et al., 2001). Oleszak and Krasnowski synthesized FeAl-Al_2O_3 nanocomposite by mechanochemical reaction of Fe_2O_3+4Al powder mixture (Oleszak & Krasnowski, 2001). They reported the average crystallite size of 10 nm after ball milling and 40-50 nm after subsequent annealing. Khodaei et al. investigated the mechanochemical synthesis of Fe_3Al-Al_2O_3 with different vol.% of Al_2O_3 (Khodaei et al., 2008), (Khodaei et al., 2009a), (Khodaei et al., 2009b). The thermodynamic consideration based on the theoretical adiabatic temperature, T_{ad}, associated with different reactions between Fe_2O_3, Al, and Fe, has revealed the modality of the mechanochemical reaction. Fe_3Al-Al_2O_3 nanocomposite powder containing 57vol. % Al_2O_3 was synthesized by mechanochemical combustion reaction of $3Fe_2O_3$+8Al powder mixture. Combustion reaction in this system is detected by abrupt increase in vial temperature (Khodaei et al., 2009a). The combustion is also observed by opening of vial at the expected time. Fig. 14 shows the opened vial during the combustion reaction.

Fig. 14. Images of opened vial during combustion reaction of $3Fe_2O_3$+8Al powder mixture.

The XRD patterns of $3Fe_2O_3$ + 8Al powder mixture as-received and after different milling times are shown in Fig. 15. XRD patterns of powder mixture after 2 h of milling time (prior to combustion reaction) was identified as a mixture of Fe_2O_3 and Al with nanocrystalline structure. XRD patterns immediately after combustion, Fig. 15(c), showed no Fe_2O_3 and Al peaks. The diffraction lines of reaction products were identified as Al_2O_3 and Fe_3Al intermetallic compound. The results showed successfully synthesized Fe_3Al and Al_2O_3 by mechanochemical reaction of $3Fe_2O_3$ + 8Al powder mixture. In contrast, Fan et al. reported that during reaction of Fe_2O_3 and molten aluminum in $3Fe_2O_3$ + 8Al system, instead of thermodynamically predicted Fe_3Al intermetallic compound, $FeAl_2O_4$ predominately forms

(Fan et al., 2006). In order to study the distribution of phases and microstructure of Fe_3Al–Al_2O_3 nanocomposite, the produced powder after 20 h of milling time was cold pressed and then sintered at 1400 °C for 1 h. Cross-sectional micrograph of sintered specimen is shown in Fig. 16. As seen, the distribution of Fe_3Al and Al_2O_3 phases is homogeneous.

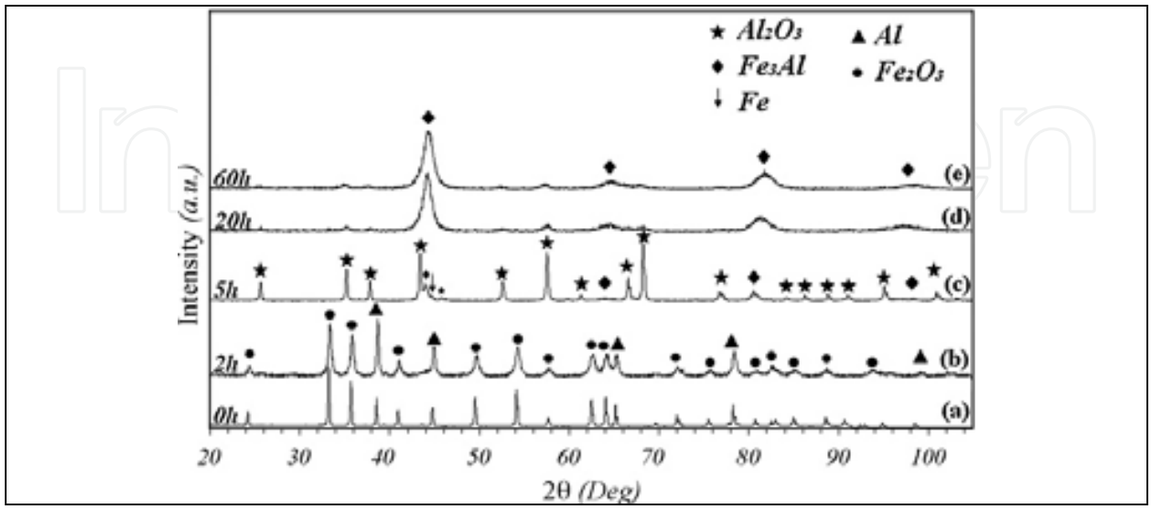

Fig. 15. XRD patterns of $3Fe_2O_3$ + 8Al powder mixture as-received and after different milling times (Khodaei et al., 2009a).

This ultrafine (>2μ) and uniform microstructure of metallic–ceramic phases without "core–rim" feature is resulted from ball milling process (Khodaei et al., 2009a). Khodaei et al. also synthesized Fe_3Al-30 vol.% Al_2O_3 nanocomposite by addition of Fe to Fe_2O_3+Al powder mixture. The modality of mechanochemical reaction of Fe_2O_3+Al+Fe powder mixture is determined by calculating the Tad of reaction as a gradual way (Khodaei et al., 2009b). For comparison, the Fe_3Al-30 vol.% Al_2O_3 nanocomposite was also prepared by ex situ addition of Al_2O_3 nanopowder to Fe–Al powder mixture followed by ball milling. The Fe_3Al-30 vol.% Al_2O_3 powders prepared by these two routes were consolidated in order to study the microstructure as well as mechanical properties of the samples. Cross-sectional SEM micrographs of the sintered samples are shown in Fig. 17. The distribution of Fe_3Al and Al_2O_3 phases in ex situ added Al_2O_3 sample is not homogeneous whereas for mechanochemically synthesized sample which involved in situ formation of Al_2O_3, a uniform distribution of Al_2O_3 is achieved. Moreover, the microstructure of mechanochemically synthesized sample is finer than that obtained for ex situ added Al_2O_3 sample and contains lower amount of porosity (Khodaei et al., 2009b). Subramanian et al. synthesized the Fe_3Al–20 vol.% Al_2O_3 composite via reactive sintering of Fe_2O_3 and FeAl powder mixture by pressureless sintering (Subramanian et al., 1997) and hot pressing (Subramanian et al., 1998) had a foam-type feature in which the Al_2O_3 phase are formed as rings around the Fe_3Al matrix (Fig. 18), probably from a reaction of FeAl and Fe_2O_3 located along the grain boundaries. These results show that the microstructure of Fe_3Al–Al_2O_3 composite produced by mechanochemical process has better characteristics compared to other processing routes. Evaluation of the mechanical properties of consolidated samples included the determination of hardness and fracture stress by three-point flexure testing at room temperature. These values for mechanochemically synthesized and ex situ added Al_2O_3 samples produced by Khodaei et al. compared with reactive sintered samples

produced by Subramanian et al. are given in Table 4. As can be seen, the hardness and fracture strength values of mechanochemically synthesized nanocomposite are higher than those produced by other methods.

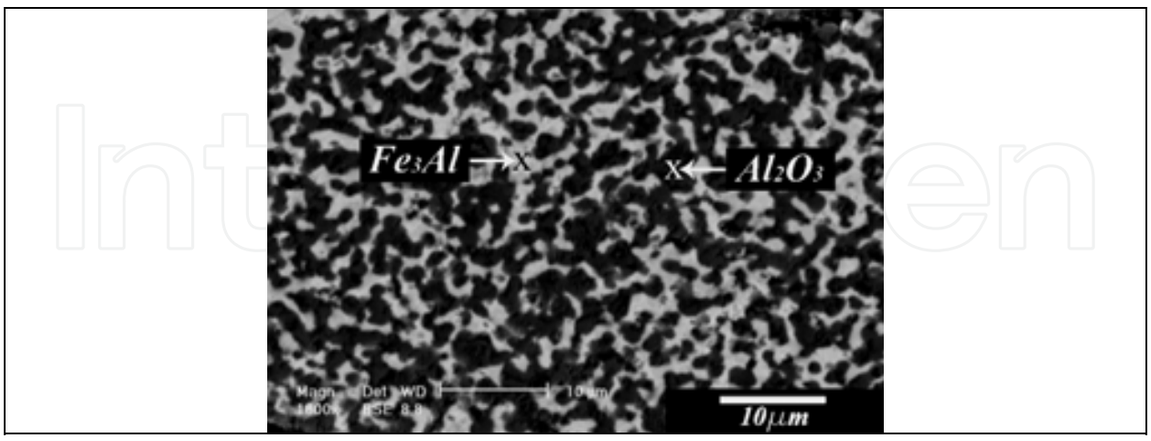

Fig. 16. SEM cross-sectional microstructure of consolidated Fe_3Al– 57 vol.% Al_2O_3 nanocomposite powder prepared by mechanochemical reaction (Khodaei et al., 2009a).

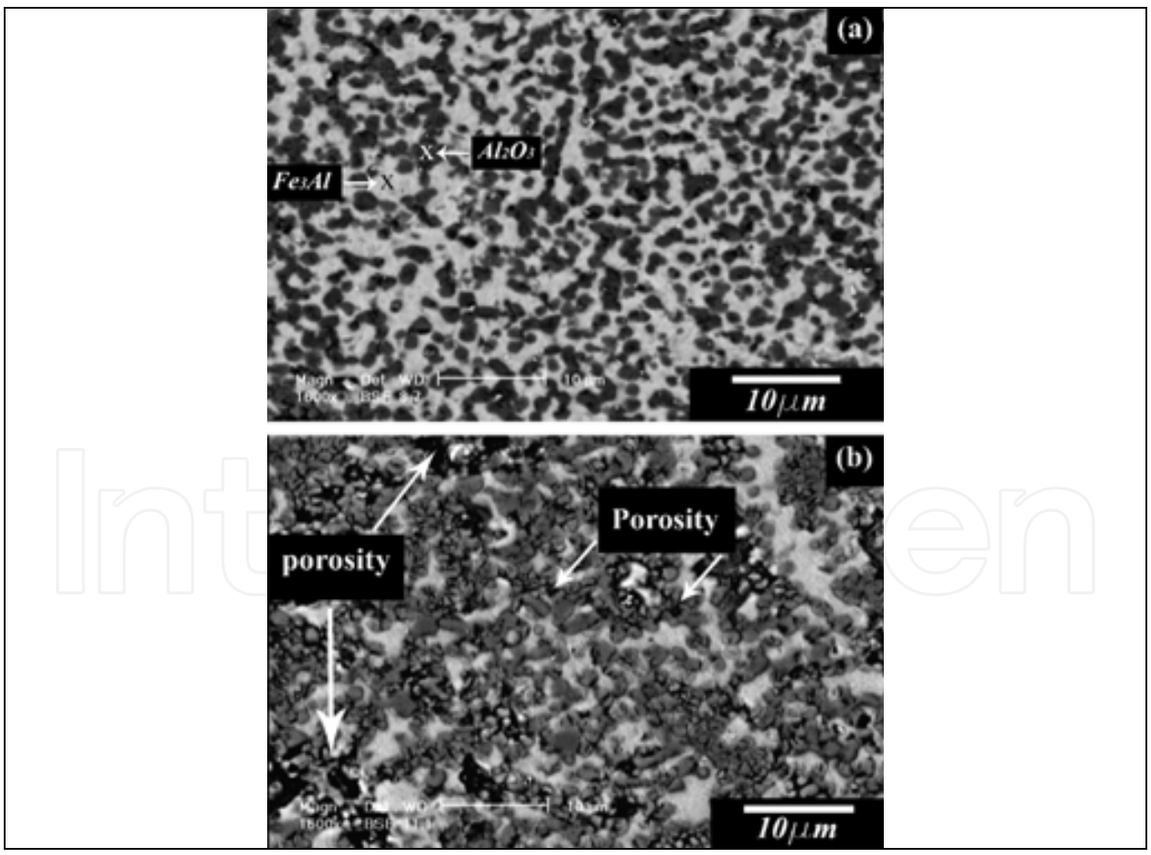

Fig. 17. SEM cross-sectional microstructure of consolidated Fe_3Al– 30 vol.% Al_2O_3 nanocomposite powder prepared by: (a) mechanochemically synthesized (b) ex situ added Al_2O_3 followed by ball milling. (Khodaei et al., 2009b).

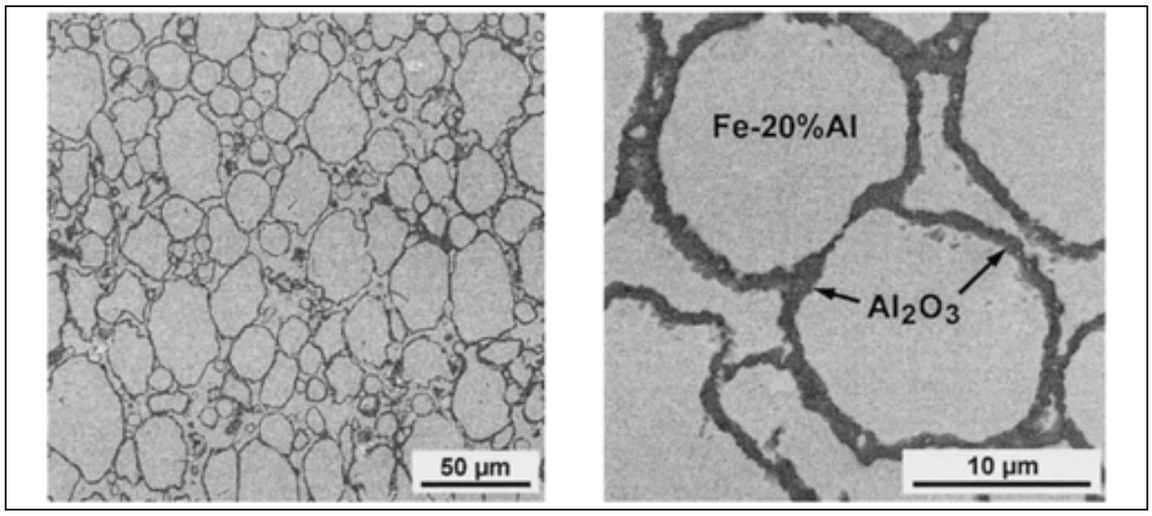

Fig. 18. SEM micrographs of an Fe_3Al-20 vol.% Al_2O_3 processed by an in situ displacement reaction via reactive sintering (Subramanian et al., 1998).

Composition	Fabrication route of Al_2O_3	Hardness (Hv)	Fracture stress (MPa)
Fe_3Al–30 vol.% Al_2O_3	Mechanochemical	538 ± 20	173 ± 9
Fe_3Al–30 vol.% Al_2O_3	Al_2O_3 nanopowder	490 ± 42	43 ± 6
Fe_3Al	–	378 ± 19	Not tested
Fe_3Al–20 vol.% Al_2O_3	Reactive sintering	222[a]	107[a]
Fe_3Al–20 vol.% Al_2O_3	Reactive sintering	355 ± 30	184 ± 2
Fe_3Al	–	308 ± 5	896[a]

Table 4. Vicker's hardness and room temperature three-point fracture stress of Fe_3Al-Al_2O_3 samples prepared by different routs (Khodaei et al., 2009b).

Rafiei et al. (Rafiei et al., 2009) reported the synthesizing $(Fe,Ti)_3Al$–Al_2O_3 nanocomposite by mechanochemical reaction in Fe+Al+TiO_2 powder mixture. Addition of third alloying element such as Ti and Cr to Fe_3Al intermetallic compound can lead to the improvement of mechanical properties. They found that the TiO_2 is gradually reduced by Al during milling. This reaction led to the formation of crystalline Ti and amorphous Al_2O_3. On further milling Ti (reduced from TiO_2) and remaining Al dissolved into Fe lattice and formed a Fe(Al,Ti) solid solution which transformed to $(Fe,Ti)_3Al$ intermetallic compound with disordered DO3 structure at longer milling times. Annealing of final structure led to the crystallization of amorphous Al_2O_3 and ordering of $(Fe,Ti)_3Al$ matrix.

Forouzanmehr et al. (Forouzanmehr et al., 2009) reported the synthesis TiAl-Al_2O_3 nanocomposite by mechanochemical reaction of TiO_2 and Al and subsequent annealing. They found that titanium oxide is gradually reduced by Al during milling. The Al(Ti) solid solution formed at the early stage of milling. Diffusion of Ti into Al is found to be dominant process. Fig. 19 shows TEM micrographs and SAD pattern of the powder milled for 60 h followed by annealing at 900°C. Fig. 19(a) displays the bright field micrograph and Fig. 19(b) shows dark field micrograph indicating nano-sized phases with less than 50 nm. The SAD pattern, Fig. 19(c), also indicates fine crystalline size as well as the absence of preferred orientation. They also reported the good agreement regarding the grain size of the phases estimated from TEM observation and that from XRD analysis using Williamson–Hall method.

Zakeri et al. for the first time reported the mechanochemically synthesized $MoSi_2$–Al_2O_3 nanocomposite by ball milling of mixture of MoO_3, SiO_2 and Al powder (Zakeri et al., 2007). They found that this reaction proceeds trough the combustion mechanochemical reaction. $NbAl_3$–Al_2O_3 nanocomposite powder with 40 vol.% Al_2O_3 was also directly synthesized by Mostaan et al. (Mostaan et al., 2010b) using mechanochemical reaction between Nb_2O_5 and Al powders. Measurement of vial temperature, XRD analysis, and morphology changes during ball milling confirmed the occurrence of combustion reaction which led to the formation of $NbAl_3$ intermetallic compound and Al_2O_3 phase. Thermal behavior results showed that nanocomposite powders were stable during heating. XRD pattern of Nb_2O_5 and Al powder mixture as-recievd and after different milling time are shown in Fig. 20.

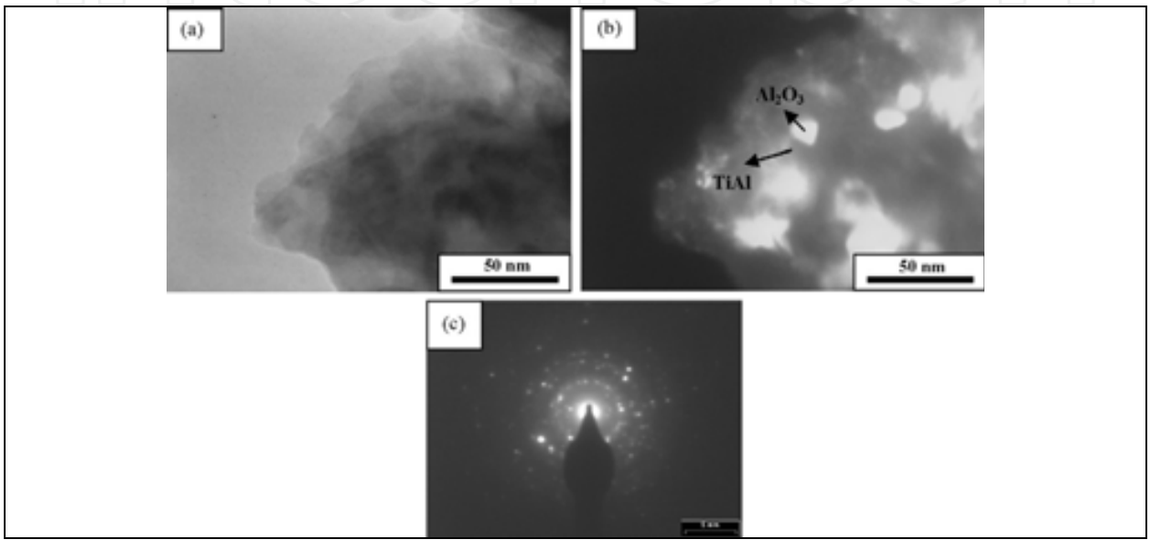

Fig. 19. TEM micrographs of TiAl-Al_2O_3 nanocomposite powder produced by milling of TiO_2+Al for 60 h followed by annealing at 900 °C: (a) Bright field, (b) Dark field, and (C) SAD pattern (Forouzanmehr et al., 2009).

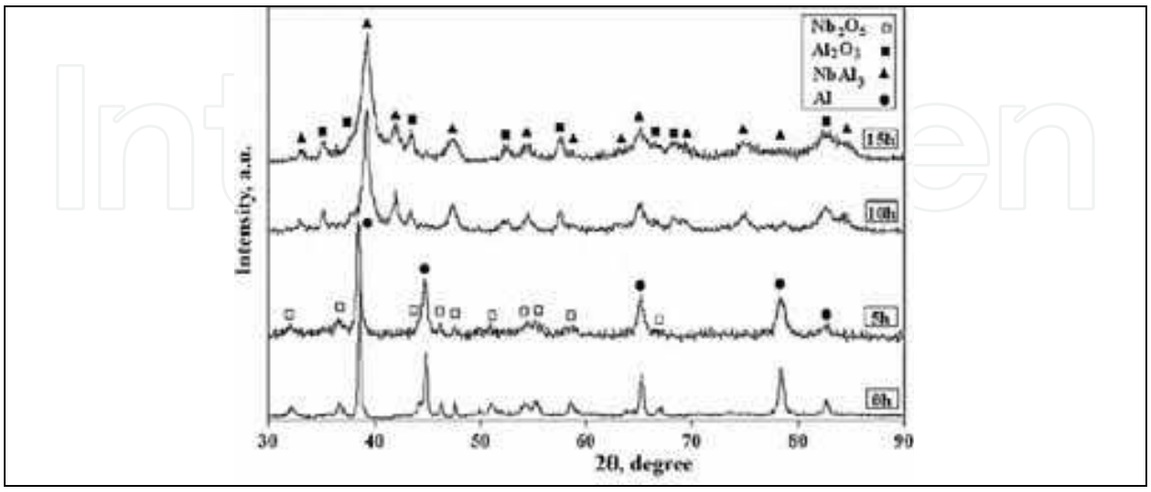

Fig. 20. XRD pattern of Nb_2O_5 and Al powder mixture as-recievd and after different milling times (Mostaan et al., 2010b)

5. Conclusion

The mechanochemical processing is a technique that could be used to synthesize composite structure which has an advantage over other fabrication route because of its capability of producing chemical compatible phase as well as nanosized structure with high uniformity. These advantages provide a useful technique for preparation of nanocomposite powder used in fabrication of advanced engineering parts trough powder metallurgy methods. The future works in this area should be done in utilizing the advanced powder metallurgy methods for consolidation of mechanochemically synthesized nanocomposite powders.

6. References

Alman, D.E.; Hawk, J.A.; Tylzak, J.H.; Dogan, C.P. & Wilson, R.D. (2001) Wear of iron-aluminide intermetallic-based alloys and composites by hard particles, *Wear*, 251, (875-884)

Anvari, S.Z.; Karimzadeh, F. & Enayati, M.H. (2009) Synthesis and characterization of NiAl–Al_2O_3 nanocomposite powder by mechanical alloying, *Journal of Alloys and Compounds,* 477, (178–181)

Arami, H.; Simchi, A. & Seyed Reihani S.M. (2008) Mechanical induced reaction in Al–CuO system for in-situ fabrication of Al based nanocomposites, *Journal of Alloys and Compounds*, 465, (151–156)

Botcharova, E.; Freudenberger, J. & Schultz, L. (2004) Mechanical alloying of copper with niobium and molybdenum, *Journal of Materials Science,* 39, (5287–5290)

Castricum H.L.; Bakker, H. & Poels, E.K. (2001) Oxidation and reduction in copper/zinc oxides by mechanical milling, Materials Science and Engineering A, 304–306, (418–423)

Chalwa, K.K. (1993) *Ceramic Matrix Composites*, 2nd ed., Chapman and Hall, USA

Chen, J.; Lu, L. & Lu K. (2006) Hardness and strain rate sensitivity of nanocrystalline Cu, *Scripta Materialia*, 54, (1913–1918)

Clyne, T.W. & Withers, P.J. (1995) *An Introduction to Metal Matrix Composites*, Cambridge, UK

Deidda, C.; Delogu, F. & Cocco, G. (2004) In situ characterization of mechanically-induced self-propagating reactions, *Journal of Materials Science*, 39, (5315-5318)

El-Eskandary, S.M. (2001) *Mechanical Alloying for Fabrication of Advanced Engineering Materials*, Noes Publication, New York

El-Eskandary, S.M.; El-Bahnasawy, N.H.; Ahmeh, H.A. & Eissa, N.A. (2001) Mechanical Solid-State Reduction of Hematite with Magnesium, *Journal of Alloys and Compounds*, 314, (286-295)

Fan, R.H.; Lu, H.L.; Sun, K.N.; Wang, W.M. & Yi, X.B. (2006) Kinetics of Thermite Reaction in Fe-Al_2O_3 System, *Thermochemica Acta*, 440, (129-131)

Forouzanmehr, N.; Karimzadeh, F. & Enayati M.H. (2009) Synthesis and characterization of TiAl/Al_2O_3 nanocomposite by mechanical alloying, *Journal of Alloys and Compounds*, 478, (257–259)

Forrester, J.S. & Schaffer, G.B. (1995) The chemical kinetics of mechanical alloying, *Metallurgical Transaction A*, 26, (725-730)

Heidarpour, A.; Karimzadeh, F. & Enayati, M.H. (2009) In situ synthesis mechanism of Al_2O_3–Mo nanocomposite by ball milling process, *Journal of Alloys and Compounds*, 477, (692–695)

Hwang, S.J.; Wexler, D. & Calika, A. (2004) Mechanochemical synthesis of nanocrystalline Al_2O_3 dispersed copper, *Journal of Materials Science*, 39, (4659–4662)

Hwang, S.J. & Lee, J. (2005) Mechanochemical synthesis of Cu–Al_2O_3 nanocomposites, *Materials Science and Engineering A*, 405, (140–146)

Karimzadeh, F.; Enayati, M.H. & Tavoosi, M. (2008) Synthesis and characterization of Zn/Al_2O_3 nanocomposite by mechanical alloying, *Materials Science and Engineering A*, 486, (45–48)

Khodaei, M.; Enayati, M.H. & Karimzadeh, F. (2008) Mechanochemical behavior of Fe_2O_3–Al–Fe powder mixtures to produce Fe_3Al–Al_2O_3 nanocomposite powder, *Journal of Materials Science*, 43, (132-138)

Khodaei, M.; Enayati, M.H. & Karimzadeh, F. (2009) Mechanochemically synthesized Fe_3Al-Al_2O_3 nanocomposite, *Journal of Alloys and Compounds*, 467, (159-162) a

Khodaei, M.; Enayati, M.H. & Karimzadeh, F. (2009) The structure and mechanical properties of Fe_3Al-30 vol.% Al_2O_3 nanocomposite , *Journal of Alloys and Compounds*, 488, (134-137) b

Konopka, K. & Szafran, M. (2006) Fabrication of Al_2O_3–Al composites by infiltration method and their characteristic, *Journal of Materials Processing Technology,* 175, (266–270)

Li J.; Ni, X. & Wang, G., (2007) Microstructure and magnetic properties of Co/Al_2O_3 nanocomposite powders, *Journal of Alloys and Compounds*, 440, (349–356)

Lin, C.K.; Hong, S.S. & Lee, P.Y. (2000) Formation of NiAl-Al_2O_3 intermetallic-matrix composite powders by mechanical alloying technique, *Intermetallics*, 8, (1043-1048)

Matteazzi, P. & Caër, G.L. (1992) Synthesis of nanocrystalline alumina-metal composites by room temperature ball milling of metal oxides and aluminum, *Journal of the American Ceramic Society*, 75, (2749-2755)

McCormick, P.G.; Wharton, V.N. & Schaffer, G.B. (1989) In: *Physical chemistry of powder metals production and processing*, Small, W.M. (19-34), TMS, Warrendale, PA

McCormick, P.G. (1995) Application of mechanical alloying to chemical refining, *Material. Transaction JIM*, 36, (161-173)

McCormick, P.G. & Froes, F.H. (1998) The fundamentals of mechanochemical processing, *Journal of Metals*, 50, (61-73)

Mishra, R.S. & Mukherjee, A.K. (2001) Processing of high hardness-high toughness alumina matrix nanocomposite, *Materials Science and Engineering A*, 301, (97–101)

Morris, D.G. (1998) Possibilities for high-temperature strengthening in iron aluminides, *Intermetallic*, 6, (753-758)

Mostaan, H.; Abbasi, M.H. & Karimzadeh, F. (2010) Mechanochemical assisted synthesis of Al_2O_3/Nb nanocomposite by mechanical Alloying, *Journal of Alloys and Compounds*, 493, (609–612) a

Mostaan, H.; Abbasi, M.H. & Karimzadeh, F. (2010) Investigation of in-situ synthesis of $NbAl_3$/Al_2O_3 nanocomposite by mechanical alloying and its formation mechanism, *Journal of Alloys and Compounds*, 503, (294–298) b

Mostaan, H.; Abbasi, M.H. & Karimzadeh, F. (2010) Non-isothermal kineticstudiesontheformationof Al_2O_3/Nb composite, *Thermochimica Acta*, (In Press) c

Mousavi, T.; Karimzadeh, F. & Abbasi, M.H. (2009) Mechanochemical assisted synthesis of NiTi intermetallic based nanocomposite reinforced by Al_2O_3, *Journal of Alloys and Compounds*, 467, (173–178)

Munir, Z.A. (1988) Synthesis of high temperature materials by self propagating combustion methods, *American Ceramic Society Bulletin*, 67, (342-349)

Oleszak, D. & Krasnowski, M. (2001) Mechanically alloyed nanocrystalline intermetallic matrix composite reinforced with alumina, *Materials Science Forum*, 360-362, (235-240)

Oleszak, D. (2004) NiAl-Al_2O_3 Intermetallic matrix composite prepared by reactive milling and consolidation of powder, *Journal of Materials Science*, 39,(5169-5174)

Piggott, M.A. (1980) *Load Bearing Fiber Composites*, Pergamon Press, London

Rafiei, M.; Enayati, M.H. & Karimzadeh, F. (2009) 59 Mechanochemical synthesis of $(Fe,Ti)_3Al$–Al_2O_3 nanocomposite, *Journal of Alloys and Compounds*, 488, (144–147)

Rajkovic, V.; Bozic, D. & Jovanovic, M.T. (2008) Properties of copper matrix reinforced with nano- and micro-sized Al_2O_3 particles, *Journal of Alloys and Compounds*, 459 (177–184)

Rajkovic, V.; Bozic, D. & Jovanovic, M.T. (2008) Properties of copper matrix reinforced with various size and amount of Al_2O_3 particles, *journal of materials processing technology*, 200, (106–114)

Reddy, B.S.B.; Das, K.; Pabi, S.K. & Das, S. (2007) Mechanical–thermal synthesis of Al–Ce/Al_2O_3 nanocomposite powders, *Materials Science and Engineering A*, 445–446, (341–346)

Sabooni, S.; Mousavi, T. & Karimzadeh, F. (2010) Mechanochemical assisted synthesis of Cu(Mo)/Al_2O_3 nanocomposite, *Journal of Alloys and Compounds*, 497, (95–99)

Sauthoff, G. (1995) *Intermetallics,* VCH, Germany

Schaffer, G.B. & McCormick, P.G. (1989) ,Applied Physics Letter, 55, (45-46)

Schaffer, G.B. & McCormick P.G. (1990) Displacement Reactions during Mechanical Alloying, *Metallurgical Transaction A*, 21, (2789-2794)

Schaffer, G.B. & McCormick, P.G. (1991) Anomalous combustion effect during mechanical alloying, *Metallurgical Transaction A*, 22, (3019–3024)

Schmalzried, H. (1995). *Chemical Kinetics of Solids,* Wiley-VCH, Weinheim

Sheibani, S.; Khakbiz, M. & Omidi, M. In situ preparation of Cu–MnO nanocomposite powder through mechanochemical synthesis, *Journal of Alloys and Compounds*, 477, (683–687)

Shengqi, X.; Xiaoyan, Q.; Mingliang, M.; Jingen, Z.; Xiulin, Z. & Xiaotian, W. (1998) Solid-state reaction of Al/CuO couple by high-energy ball milling, *Journal of Alloys and Compounds*, 268, (211–214)

Stein, A.; Keller, S.W. & Mallouk, T.E. (1993) Turning down the heat: design and mechanism in solid-state synthesis. *Science*, 259, (1558-1564)

Subramanaian, R.; McKamery, G.C.; Buck, L.R. & Schneilbel, J.H. (1997) Synthesis of iron aluminide–Al_2O_3 composites by in situ displacement reaction, *Materials Science and Engineering A*, 239-240, (640-646)

Subramanaian, R.; McKamery, G.C.; Schneilbel, J.H. & Menchhofer, P.M (1998) Iron aluminide–Al_2O_3 composites by in situ displacement reactions: processing and mechanical properties, *Materials Science and Engineering A*, 254, (119-128)

Suryanarayana, C. (2001) Mechanical alloying and milling, *Progress in Materials Science*, 46, (1-184)

Takacs, L. (2002) Self-sustaining reaction induced by ball milling, *Progress in Materials Science*, 47, (355-414)

Tavoosi, M.; Karimzadeh, F. & Enayati, M.H. (2008) Fabrication of Al–Zn/α-Al_2O_3 nanocomposite by mechanical alloying, *Materials Letters,* 62, (282–285)

Tavoosi, M.; Karimzadeh, F.; Enayati, M.H. & Heidarpour, A. Bulk Al–Zn/Al_2O_3 nanocomposite prepared by reactive milling and hot pressing methods, *Journal of Alloys and Compounds*, 475, (198–201)

Udhayabanu, V.; Ravi, K.R.; Vinod, V. & Murty, B.S. (2010) Synthesis of in-situ NiAl–Al_2O_3 nanocomposite by reactive milling and subsequent heat treatment *Intermetallics*, 18, (353–358)

Wu, J.M. & Li, Z.Z. (2000) Nanostructured composite obtained by mechanically driven reduction reaction of CuO and Al powder mixture, *Journal of Alloys and Compounds*, 299, (9–16)

Ying, D.Y. & Zhang, D.L. (2000) Processing of Cu–Al_2O_3 metal matrix nanocomposite materials by using high energy ball milling, *Materials Science and Engineering A*, 286, (152–156)

Ying, D.Y. & Zhang, D.L. (2000) Solid state reactions between CuO and Cu(Al) or Cu_9Al_4 in mechanically milled composite powders, *Materials Science and Engineering A*, 361, (321–330)

Zakeri, M.; Yazdani-Rad, R.; Enayati, M.H.; Rahimipour, M.R. & Mobasherpour, I. (2007) Mechanochemical reduction of MoO_3/SiO_2 powder mixtures by Al and carbon for the synthesis of nanocrystalline $MoSi_2$, *Journal of Alloys and Compounds*, 430, (170–174)

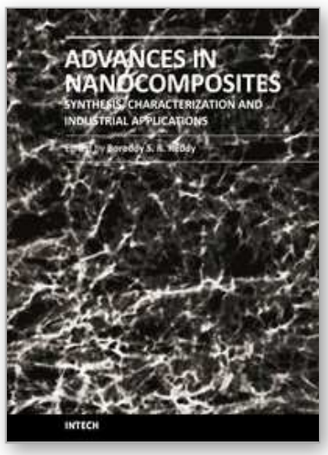

Advances in Nanocomposites - Synthesis, Characterization and Industrial Applications

Edited by Dr. Boreddy Reddy

ISBN 978-953-307-165-7
Hard cover, 966 pages
Publisher InTech
Published online 19, April, 2011
Published in print edition April, 2011

Advances in Nanocomposites - Synthesis, Characterization and Industrial Applications was conceived as a comprehensive reference volume on various aspects of functional nanocomposites for engineering technologies. The term functional nanocomposites signifies a wide area of polymer/material science and engineering, involving the design, synthesis and study of nanocomposites of increasing structural sophistication and complexity useful for a wide range of chemical, physicochemical and biological/biomedical processes. "Emerging technologies" are also broadly understood to include new technological developments, beginning at the forefront of conventional industrial practices and extending into anticipated and speculative industries of the future. The scope of the present book on nanocomposites and applications extends far beyond emerging technologies. This book presents 40 chapters organized in four parts systematically providing a wealth of new ideas in design, synthesis and study of sophisticated nanocomposite structures.

How to reference

In order to correctly reference this scholarly work, feel free to copy and paste the following:

M. Khodaei, M.H. Enayati and F. Karimzadeh (2011). Mechanochemically Synthesized Metallic-Ceramic Nanocomposite; Mechanisms and Properties, Advances in Nanocomposites - Synthesis, Characterization and Industrial Applications, Dr. Boreddy Reddy (Ed.), ISBN: 978-953-307-165-7, InTech, Available from: http://www.intechopen.com/books/advances-in-nanocomposites-synthesis-characterization-and-industrial-applications/mechanochemically-synthesized-metallic-ceramic-nanocomposite-mechanisms-and-properties

INTECH
open science | open minds

InTech Europe
University Campus STeP Ri
Slavka Krautzeka 83/A
51000 Rijeka, Croatia
Phone: +385 (51) 770 447
Fax: +385 (51) 686 166
www.intechopen.com

InTech China
Unit 405, Office Block, Hotel Equatorial Shanghai
No.65, Yan An Road (West), Shanghai, 200040, China
中国上海市延安西路65号上海国际贵都大饭店办公楼405单元
Phone: +86-21-62489820
Fax: +86-21-62489821

IntechOpen